Physical Oceanography of the SW Atlantic Shelf: A Review

Alberto R. Piola, Elbio D. Palma, Alejandro A. Bianchi, Belmiro M. Castro, Marcelo Dottori, Raul A. Guerrero, Marina Marrari, Ricardo P. Matano, Osmar O. Möller Jr, and Martín Saraceno

Abstract The continental shelf of the western South Atlantic is characterized by three regions subject to distinct oceanographic regimes. The wide subantarctic shelf, south of approximately 35°S, is occupied by cold, low-salinity waters derived from the Subantarctic Zone and further diluted by the inflow of additional low-salinity waters, primarily from the Magellan Strait. Farther north, the shelf narrows considerably and is subject to the influence of large freshwater discharges and warm-salty intrusions of subtropical waters from the Brazil Current. Intense frontal transitions at various near shore locations and along the shelf break promote vertical circulations that inject nutrients into the upper layer. This nutrient injection leads to

A. R. Piola (✉) · A. A. Bianchi
Departamento Oceanografía, Servicio de Hidrografía Naval (SHN),
Ciudad Autónoma de Buenos Aires, Argentina

Departamento de Ciencias de la Atmósfera y los Océanos, Universidad de Buenos Aires,
Ciudad Autónoma de Buenos Aires, Argentina
e-mail: apiola@hidro.gov.ar; abianchi@hidro.gov.ar

E. D. Palma
Instituto Argentino de Oceanografía (IADO-CONICET), Consejo Nacional de
Investigaciones Científicas y Técnicas and Depatamento de Física, Universidad Nacional del
Sur, Bahía Blanca, Argentina
e-mail: uspalma@criba.edu.ar

B. M. Castro · M. Dottori
Instituto Oceanográfico, Universidade de São Paulo, São Paulo, Brazil
e-mail: bmcastro@usp.br; mdottori@usp.br

R. A. Guerrero
Instituto Nacional de Investigación y Desarrollo Pesquero (INIDEP), Mar del Plata, Argentina
e-mail: raul.guerrero@inidep.edu.ar

M. Marrari
Departamento Oceanografía, Servicio de Hidrografía Naval (SHN),
Ciudad Autónoma de Buenos Aires, Argentina
e-mail: mmarrari@hidro.gov.ar

enhanced growth of phytoplankton, and, in some regions, to a significant uptake of atmospheric CO_2. While the subantarctic shelf is under the influence of strong westerlies and high-amplitude tides, most of the subtropical shelf undergoes seasonally reversing winds and a micro-tidal regime. The shelf characteristics are also influenced by the offshore circulation, which is dominated by the equatorward flow of cold, nutrient-rich waters of the Malvinas Current in the south and the poleward flow of warm, salty, and oligotrophic waters of the Brazil Current in the north. There is a convergent large-scale mean circulation toward the transition between subantarctic and subtropical shelf waters near 34°S, which is balanced by export of shelf waters to the deep ocean. This article describes the contrasting water masses, frontal features, and circulation patterns of this region.

Keywords Ocean circulation · Water masses · Ocean fronts · Western South Atlantic shelf

1   Introduction

The portion of the continental shelf of eastern South America between Cape Frío (23°S) and Tierra del Fuego (55°S) is characterized by distinct morphological, climatic, and oceanographic features. This 4300-km-long shelf region encompasses three distinct subregions: the Patagonia continental shelf (PS) (38°S–55°S) to the south; the central shelf (CS), which includes portions of the southern Brazil, Uruguay, and northern Argentina shelves and extends from Cape Santa Marta Grande to Cape Corrientes (28°S–38°S); and the South Brazil Bight (SBB) to the north (23°S–28°S). South of 38°S, the continental shelf is a wide plateau subject to intense westerly winds and high tidal variability. The PS is bounded offshore by the

R. P. Matano
College of Earth, Ocean, and Atmospheric Sciences, Oregon State University,
Corvallis, OR, USA
e-mail: rmatano@coas.oregonstate.edu

O. O. Möller Jr
Instituto de Oceanografia, Universidade Federal do Rio Grande, Rio Grande, Brazil
e-mail: dfsomj@furg.br

M. Saraceno
Departamento de Ciencias de la Atmósfera y los Océanos, Universidad de Buenos Aires,
Ciudad Autónoma de Buenos Aires, Argentina

Centro de Investigaciones del Mar y la Atmósfera, Consejo Nacional de Investigaciones
Científicas y Técnicas–Universidad de Buenos Aires, Ciudad Autónoma de Buenos Aires,
Argentina
e-mail: saraceno@cima.fcen.uba.ar

cold, nutrient-rich and relatively fresh waters from the Antarctic Circumpolar Current along the southern boundary, which are advected northward by the Malvinas Current (MC) to about 38°S along the western boundary of the Argentine Basin. Farther north, there is the CS, which is 1350 km long and significantly narrower than the other two shelf regions, reaching about 80 km off Mostardas, near 31°16'S. The CS is strongly influenced by the continental discharge of the Río de la Plata (RP) and the Patos/Mirim Lagoon, and by its proximity to the Brazil Current (BC) and the Brazil/Malvinas Confluence, which bound its offshore limit and promote energetic exchanges between shelf and deep ocean waters. The SBB is a 1000-km-long crescent-shaped bay approximately 200 km wide at the center and 70–80 km at its northern and southern boundaries. This region is bounded offshore by the southward-flowing BC, the western boundary current of the Subtropical Gyre, which exerts a significant influence on the shelf circulation, biology, and biogeochemistry. This chapter describes the water mass, chlorophyll a and CO_2 flux distributions, and circulation over the continental shelf of these three shelf regions.

2 Data and Methods

For this review we have analyzed historical hydrographic data from holdings at INIDEP, Argentina (http://www.inidep.edu.ar/oceanografia/PERFILES/); CEADO, Argentina (http://www.hidro.gov.ar/ceado/ceado.asp); NOAA's National Centers for Environmental Prediction World Ocean Data (https://www.nodc.noaa.gov/OC5/WOD/pr_wod.html); and Argo profiling float data (http://www.argo.ucsd.edu/). These data were combined to prepare the updated sea surface salinity distribution presented in Fig. 1a. The hydrographic data are also used to prepare seasonal vertical temperature differences in the upper layer. In addition, we analyzed satellite-derived sea surface temperature (SST) and chlorophyll concentration data. We used NOAA's Optimum Interpolated SST version 2.0 with daily $0.25 \times 0.25°$ resolution (Reynolds et al. 2007, available at https://www.ncdc.noaa.gov/oisst) to estimate sea surface temperature gradients presented in Fig. 1b. Surface chlorophyll a concentration data are derived from MODIS Aqua collected during 2002–2017. All level 2 data were processed to construct the austral summer climatology of 2 km × 2 km resolution presented in Fig. 1c using the OC3 algorithm (O'Reilly et al. 2000). The data were made available by NASA's Ocean Biology Processing Group at the Goddard Space Flight Center. Only chlorophyll a data with concentrations within the 0.02–30 mg m^{-3} range were used in the present analyses. For further details the reader is referred to Marrari et al. (2017). The analysis of surface ocean partial pressure is carried out based on data extracted from the Surface Ocean CO_2 Atlas version 4 (SOCAT, https://www.socat.info/). These data include 130,000 observations collected from 1991 to 2015.
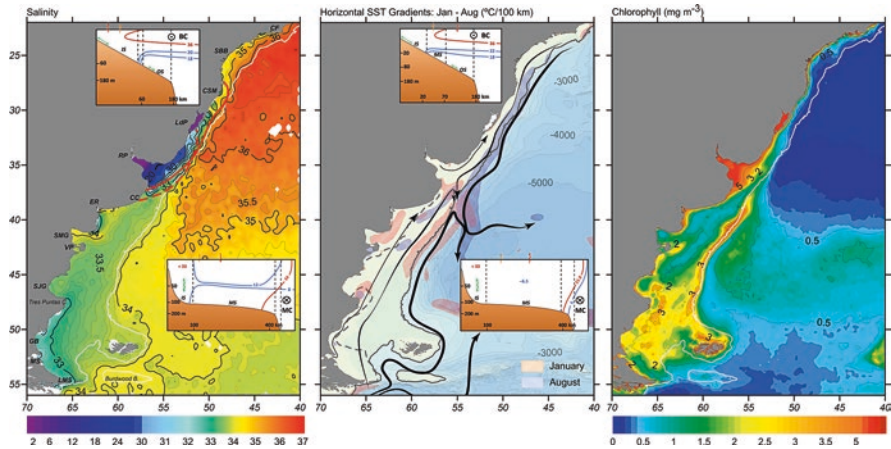
Fig. 1 Climatological sea surface salinity distribution (**a**). The red solid (dashed) contour indicates the austral winter (summer) distribution of the 33.5 isohaline, which marks the offshore edge of Plata Plume Water. CF Cape Frio, SBB South Brazil Bight, CSM Cape Santa Marta Grande, LdP Lagoa dos Patos, RP Río de la Plata, CC Cape Corrientes, ER El Rincón. SMG San Matías Gulf, VP Valdes Peninsula, SJG San Jorge Gulf, GB Grande Bay, MS Magellan Strait, LMS Le Maire Strait. The heavy white line indicates the 200 m isobath. (**b**) Mean summer (orange) and winter (blue) distributions of high sea surface temperature gradients (> 1.5 °C/100 km). The background contours show the bottom topography based on Gebco 30-second-gridded bathymetry. The heavy gray line indicates the 200 m isobath. The insets in a and b display schematic representations of the cross-shelf thermohaline structure in the SBB and the PS. The insets display selected isotherms (light blue) and isohalines (red), surface heat (red wiggly arrow), and freshwater exchanges (orange arrow). The green wiggly arrows indicate vertical mixing. In addition, a schematic surface circulation is shown, adapted from Piola and Matano (2017). (**c**) Mean summer (21 December–21 March) MODIS surface chlorophyll *a* in mg m^{-3} distribution (2002–2017). The heavy white line indicates the 200 m isobath

3 Water Masses and Shelf Fronts

3.1 *Patagonian Shelf*

In what follows we will use surface salinity, which in this region is not subject to strong seasonal fluctuations, as an identifier of water mass characteristics (e.g., Bianchi et al. 1982; Guerrero and Piola 1997; Piola et al. 2010). Figure 1a presents the climatological near-surface (0–5 meter) salinity distribution based on the analysis of 46,843 observations consisting of bottle, CTD and Argo profiles, hereafter referred to as sea surface salinity (SSS).

The southern portion of the PS is occupied by a modified type of subantarctic waters (SSS < 33.9) that enters the shelf through its southern boundary (e.g., Brandhorst and Castello 1971; Guerrero and Piola 1997). Since the PS is characterized by an excess of evaporation (~2.5 mm day^{-1}, ERA Interim, https://www.ecmwf.int/en/research/climate-reanalysis/era-interim) and only small river runoff, these low-salinity waters reflect the influence of the fresher waters advected from the

coastal regions of southern Chile, which are dominated by an excess in precipitation and continental runoff. These low-salinity waters enter the PS via the Magellan Strait (MS, SSS < 32) and the Le Maire Strait (LMS, SSS < 33) (Fig. 1). Slightly saltier waters (SSS < 33.9) enter the PS east of Estados Island. These waters, which are derived from the Cape Horn Current, are diluted along the southern coast of Chile (e.g., Dávila et al. 2002). The low salinity that emanates from the MS and LMS extends northeastward along the coast of Grande Bay, separates from the coast near Cape Tres Puntas (~47°S), and extends to the mid-shelf region at 40°S. This buoyancy plume, which Brandhorst and Castello (1971) called the Patagonian Current, merges with the low-salinity waters derived from the RP near 39°S (Fig. 1a). The Santa Cruz (790 m^3 s^{-1}), Negro, and Colorado Rivers (1160 m^3 s^{-1}) provide additional freshwater injections that form low-salinity plumes of local significance at 50°S and 40°S (Fig. 1a). Bianchi et al. (1982) defined the coastal waters as those with a SSS < 33.4, shelf waters as 33.4 < SSS < 33.8, and high-salinity shelf water due to local excess evaporation and extended residence time within San Matías Gulf, where SSS > 33.8 (Scasso and Piola 1988; Tonini et al. 2013). Although our SSS analysis is based on a substantially larger number of observations than previously reported (nearly 50% of the data in Fig. 1a were collected after the year 2000), the SSS distribution over the shelf is qualitatively similar to the one described by Bianchi et al. (2005), thus suggesting that the distribution is relatively robust. The most notable differences between our SSS distribution and earlier analyses are subtle: a farther northward extension of the Magellan plume (SSS < 33.6), which merges with the RP plume, and the high-salinity shelf water from San Matías Gulf, which occupies a wider portion of the inner shelf off El Rincón (Fig. 1a). The salty waters derived from the San Matías Gulf extend northeastward during fall–winter and are located east of the gulf's mouth in spring–summer (Lucas et al. 2005). As will be discussed later, the seasonal wind variability is a dominant forcing of the circulation over the shelf north of about 39°S.

The PS hosts a variety of ocean fronts: upwelling, tidal, shelf break, and cold and temperate estuarine fronts, all of which play a significant ecological role (Acha et al. 2004; Sabatini et al. 2004). The most prominent of these fronts is the shelf break front, which marks the limit between the relatively warm and fresh waters on the shelf from the colder and saltier MC waters. From austral spring to autumn, the shelf break front is readily detected by satellite infrared observations (e.g., Martos and Piccolo 1988; Saraceno et al. 2004; Franco et al. 2008; Rivas and Pisoni 2010). During these seasons, the thermal structure of the shelf break front reveals a transition from the stratified shelf waters to the less stratified waters farther offshore (e.g., Romero et al. 2006). The regional extent of the weakening thermal manifestation of the shelf break front in winter is due to weak thermal stratification over the shelf (<0. 5 °C) compared to the summer stratification (>6 °C, Fig. 2).

Near coastal fronts develop primarily in the summer (Rivas and Pisoni 2010, Fig. 1b). These fronts mark the transition between well-mixed coastal waters and stratified mid-shelf waters (Glorioso 1987, Fig. 2). Tidal-induced mixing is one of the main mechanisms generating these fronts, which are characterized by their sharp SST signature (Palma et al. 2004). The most notable of these fronts are located
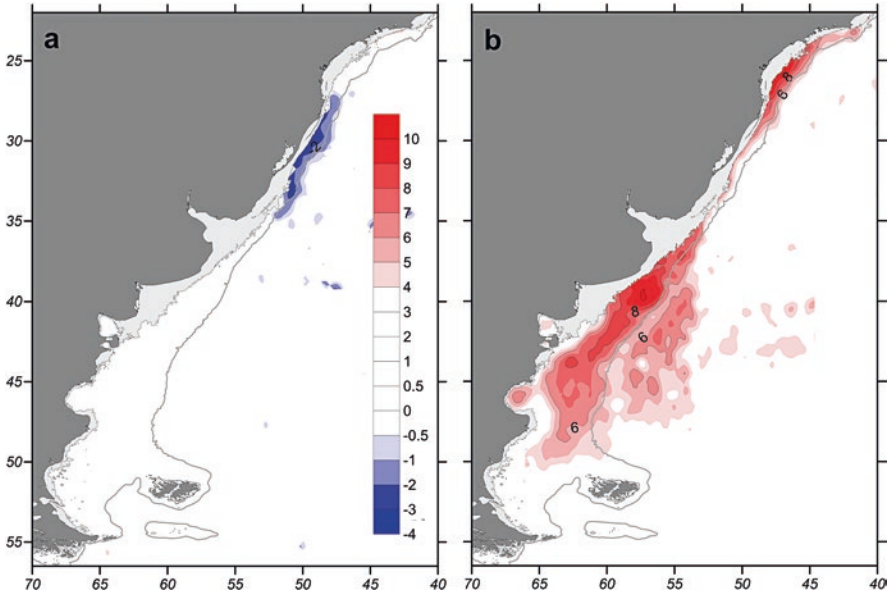
Fig. 2 Temperature difference (°C) between upper layer (10 m) and lower layer (65 m) from historical data collected during (**a**) austral winter (July–September) and (**b**) summer (December–March). Note that only positive temperature differences (T at 10 m > T at 65 m) larger than 4 °C are colored.

at ~47–50°S and along the mouth of San Matías Gulf (~42°S) (Palma et al. 2008; Moreira et al. 2011; Tonini et al. 2013). Tidal mixing is also intense along the coast south of 51°S, but the weak thermal stratification in the mid-shelf region (Fig. 2a and inset in Fig. 1a) leads to weaker thermal gradients. This region, which is characterized by the penetration of the Magellan Strait's buoyant plume and minor contributions from small rivers, is considered a cold estuarine front (Acha et al. 2004). The low-salinity waters, which extend approximately100 km offshore, are moderately warmer/colder than the mid-shelf waters during summer/winter (Rivas and Pisoni 2010). The location of tidal fronts is generally stable although frontal displacements are modulated by the intensity of surface heat flux, the fortnightly tidal cycle, and local mesoscale variability (Pisoni et al. 2015).

3.2   Central Shelf (CS)

The water mass structure of the CS is dominated by the presence of subantarctic shelf waters (SASW) with salinities between 33.6 and 33.8 (Piola et al. 2000). This region is narrower than the PS farther south: 180 km at 38°S, 110 km at 34.5°S, and just under 100 km at 31°S. The oceanic circulation over the CS is driven by seasonally reversing winds (e.g., Castro and Miranda 1998; Palma et al. 2008), which have a substantial

imprint on the local water mass distribution on account of their influence on the RP plume (e.g., Piola et al. 2000; Simionato et al. 2001, 2010; Palma et al. 2008; Saraceno et al. 2014; Matano et al. 2014; Strub et al. 2015). Thus, the annual mean SSS distribution in the CS should be interpreted with caution. RP, the second largest river of the southern hemisphere, has an average volume discharge of 23,000 m^3 s^{-1} during 1931–2016, although this value has increased to 25,000 m^3 s^{-1}during the past few decades (1997–2016) (Borús et al. 2017). The seasonal variations in RP discharge are small, but its interannual variations are significant due to the impact of El Niño on regional rainfall (Depetris et al. 1996; Robertson and Mechoso 1998). The strong Niños of 1983 and 1998, for example, generated discharges larger than 70,000 m^3 s^{-1}. These discharges had a significant impact on the SSS and on the biological and biogeochemical characteristics of the continental shelves of Uruguay and southern Brazil (Ciotti et al. 1995). During the austral fall and winter, the RP plume extends beyond the Cape Santa Marta Grande, near 28°S. In late spring and summer, the plume retracts southward, with its northern limit at approximately the mouth of the Patos Lagoon (32°S) and its southern limit near 38°S (Piola et al. 2000, 2005, 2008b; Möller Jr et al. 2008) (Fig. 1a). Events of strong southwesterly winds and large river outflow lead to exceptionally larger northeastward penetrations of the river plume (Piola et al. 2005). Such events exert a strong biological impact in the coastal areas (Stevenson et al. 1998; Proença et al. 2017). Nagai et al. (2014) show that the RP is the major source of terrigenous sediments for shelf areas between 38 and 27°S and only strong northeasterly winds can reverse this northward flow (Zavialov et al. 2002). Lateral mixing between RP waters and Tropical (TW) and South Atlantic Central waters (SACW) of the BC forms the subtropical shelf waters (Piola et al. 2000, 2008a). During the spring and summer seasons, northeasterly winds push the plume waters toward the south and offshore (Möller Jr et al. 2008; Guerrero et al. 2014; Matano et al. 2014), and most of the northern portion of the CS is occupied by subtropical shelf waters and tropical and central waters derived from the BC (see Souza and Robinson 2004). Under these summer conditions, upwelling events are frequently observed south of Cape Santa Marta Grande (Campos et al. 2013). Similarly, coastal bands of negative sea surface temperature anomalies observed along the southern coast of Uruguay are indicative of upwelling associated with strong easterly winds (e.g., Palma et al. 2008; Pimenta et al. 2008; Simionato et al. 2010). These events are also evident as bands of low coastal sea level in satellite-derived sea surface height anomalies and tide gauge data (Saraceno et al. 2014).

Satellite SST data show two distinct shelf break fronts in the region between 45°S and 25°S (Fig. 1b). South of 38°S the shelf break front marks the transition between the SASW and the cold subantarctic waters within the MC (see Sect. 3.1). In the northern region, the shelf break front marks the transition between the warm BC waters and the relatively colder shelf waters. The SST gradient between these regions is most intense during the austral winter (Fig. 1b; Saraceno et al. 2004), when there is a larger northward penetration of cold subantarctic waters flowing from the southern portion of the CS. The opposing flows reinforce the strong thermohaline gradients in the outer shelf (e.g., Möller Jr et al. 2008; Piola et al. 2008a; Matano et al. 2014). The strong cross-shelf temperature gradients can effectively

modulate the atmospheric boundary layer and the surface wind field (Mendonça et al. 2017). In winter on the mid- and outer shelf, the cold subantarctic waters combined with the cold Plata plume waters frequently overlie warm-salty waters influenced by the Brazil Current, creating a sharp thermal inversion over the northern portion of CS (Fig. 2a), which has been referred to as the inverted thermocline (Castello and Möller 1977).

The second most remarkable of the shelf fronts in the southwestern Atlantic region—after the Patagonia shelf break front—is the Subtropical Shelf Front (STSF), which marks the subsurface limit between the SASW and the STSW (Piola et al. 2000, 2008a). The STSF extends from the inner shelf at around 32°S nearly to 36°S at the shelf break (see Fig. 10 in Piola et al. 2008a). In winter, the density structure is mostly controlled by the salinity distribution preventing isopycnal mixing across the STSF, while in summer the strong thermocline provides common isopycnal layers, allowing cross-front mixing (Piola et al. 2008a).

3.3 South Brazil Bight (SBB)

The southward-flowing BC sweeps the continental slope of the SBB, although only a small fraction of it intrudes on the outer shelf region (Silveira et al. 2000). This western boundary current transports TW (T > 20 °C; S > 36) in the mixed layer and SACW (T < 20 °C; 35 < S < 36) in the pycnocline layer (Emilsson 1961). The low-salinity coastal water (CW; S < 35) mostly occupies the inner shelf (Castro and Miranda 1998). Castro (2014) identified three regions with distinct thermohaline properties in the cross-shelf direction of the SBB (see insets in Fig. 1a, b): outer shelf (OS), mid-shelf (MS), and inner shelf (IS). The IS is located onshore of a bottom temperature front, also referred to as bottom thermal boundary (BTB), which is defined by the bottom intersection of the 18 °C isotherm. The BTB separates the near-bottom intrusion of SACW from the inshore mixed waters. The IS width varies seasonally between 10–30 km in summer and 40–80 km in winter. The IS waters are usually weakly stratified compared to the MS, except near the medium estuarine systems present in the SBB, and are dominated by relatively low-salinity CW. The MS is located between the BTB and a sharp surface salinity front, also referred to as surface haline boundary (SHB). The SHB is marked by the surface outcrop of the 36 isohaline which determines the transition between TW and inshore mixed waters. Along most of the SBB, the SHB is found ~ 80 km from shore in summer and 130 km in winter.

The volume of each of the three SBB water masses changes seasonally (Cerda and Castro 2014). During autumn, the volume of SACW in the SBB is approximately equal to the volume of TW, but progressively increases, reaching a maximum in summer, when it is almost twice that of the TW. The CW is the product of mixing of TW with small amounts of continental discharges within the SBB. Its volume and physical characteristics change seasonally. In summer, the volume of CW is larger than in the other seasons, but in summer the CW is somewhat saltier

(S > 34.5) than in winter. The main seasonal change in characteristics of the CW is due to northward intrusions in winter of low-salinity waters originating south of the SBB, off the RP and the Patos and Mirim Lagoons (Campos et al. 1995; Stevenson et al. 1998; Lentini et al. 2001; Piola et al. 2000; Acha et al. 2004; Möller Jr et al. 2008; Campos et al. 2013). Interannual variability of the RP intrusions is associated with large outflow events during El Niño (Campos et al. 1999) and, most importantly, with anomalous southwesterlies over the continental shelf (Piola et al. 2005).

Onshore intrusions of nutrient-rich SACW play a significant role in fertilization of the SBB (Castro et al. 2006). There are two main intrusion paths: local, when the oceanic water reaches the MS directly from the shelf break, and remote, when SACW intrudes on the shelf at upstream regions, usually near Cape Frio, and then flows southward along the coast (Cerda and Castro 2014). Intermittent coastal upwelling events of SACW have been observed around Cape Frio, especially in spring and summer, when the region is under the influence of strong and persistent easterly and northeasterly winds (Miranda 1985; Franchito et al. 2008).

Other processes also contribute to the development of upwelling events. Rodrigues and Lorenzetti (2001) showed that the abrupt change in the coastline orientation near Cape Frio favors the effect of wind-induced upwelling. Cerda and Castro (2014) showed that the divergence of the 100 m and 150 m isobaths near Cape Frio favors SACW intrusions toward the coast. Several studies suggested that cyclonic meanders from the BC induce upward motions that inject SACW into the OS (Campos et al. 1995; Cirano and Campos 1996; Campos et al. 2000; Castelão et al. 2004). In addition, the wind stress curl contributes to force local SACW intrusions near Cape Frio (Amor 2004; Castelão and Barth 2006; Castelão 2012). Using numerical models, Palma and Matano (2009) and Matano et al. (2010) showed that the along-shelf pressure gradient near the shelf break, generated by interactions between the BC and the continental slope topography, forces geostrophic currents toward the coast in the bottom boundary layer, elevating the isopycnals toward the sea surface and favoring the onshore penetration of SACW intrusions.

4 Circulation

4.1 Patagonian Shelf (PS)

Numerical simulations suggest that the mean circulation over the continental shelf south of 40°S consists of a broad northeastward flow that intensifies toward the outer shelf (Palma et al. 2008; Combes and Matano 2014). Short-term current records at 43°S indicate mean velocities of 5.9 cm s^{-1} at 17 m and 3.1 cm s^{-1} at 67 m (Rivas 1997) that increase toward the shelf break, reaching values of 40 cm s^{-1} at 10 m depth and 26 cm s^{-1} at 160 m depth (Valla and Piola 2015). This velocity increase is associated with the proximity of the northward-flowing MC (Palma et al. 2008). In the inner shelf, the circulation is modulated by the coastal geometry, which is characterized by the presence of several bays and gulfs. Two of the largest bays are

Grande Bay and the San Jorge Gulf. Numerical models indicate that the circulation in these regions is dominated by relatively weak anticyclonic gyres and poleward coastal currents. South of 49°S, the down shelf development of the Magellan low-salinity plume is highly influenced by tides and wind forcing (Palma and Matano 2012). The circulation features produced by models are in good agreement with geostrophic flows derived from altimeter data at seasonal scales (Ruiz-Etcheverry et al. 2016). The southern shelf exports water northward and eastward in the surface layer that is largely compensated by inflow from the south at all depths and to a lesser extent by subsurface entrainment from the MC (e.g., Combes and Matano 2014). The onshore flow of MC waters is also apparent from the frequent observation of cold-salty subsurface intrusions in the outer shelf (insets in Fig. 1a, b).

Model simulations indicate a moderate strengthening of the northeastward flow during fall and a weakening during spring. North of 48°S, these seasonal variations are mainly driven by the wind forcing over the inner and mid-shelf, while further south, and offshore of the 100 m isobath, the flow is strongly modulated by MC transport variations (Palma et al. 2008). Direct current observations are too short to display a seasonal cycle, but the altimeter-derived currents also present a seasonal pattern. However, in contrast with model results, the intensification and weakening of the altimeter circulation shift to late summer and late winter, respectively (Ruiz-Etcheverry et al. 2016).

The remarkable phytoplankton blooms of the Patagonia shelf break are symptomatic of the upwelling of deep, nutrient-rich waters to the photic zone. It has been postulated and verified using simplified models that the upwelling might be associated with frictionally driven intrusions of the MC onto the shelf (Matano and Palma 2008; Miller et al. 2011). These results have been corroborated by realistic numerical simulations (Palma et al. 2008; Combes and Matano 2014) and observational studies (Valla and Piola 2015). It has also been proposed that the observed variability of the blooms can be modulated by continental shelf waves at seasonal time scales (Saraceno et al. 2005) and by wind variability at intra-seasonal periods (< 15 days, Carranza et al. 2017).

4.2 Central Shelf (CS)

The northward mean flow derived from models extends to about 38°S. This flow strengthens during fall and weakens during spring (Palma et al. 2008; Combes and Matano 2014). The relatively weak seasonal variations predicted by models are in fairly good agreement with those from altimeter observations (Strub et al. 2015; Ruiz-Etcheverry et al. 2016). In contrast, farther north, between 38°S and 28°S, models show a general southward flow on the outer shelf, which is largely controlled by the BC. The inner and mid-shelf regions exhibit significant seasonal changes in circulation and in temperature and salinity fields (Palma et al. 2008; Combes and Matano 2014). The circulation in this region is primarily driven by the alongshore component of the wind stress, which generates a positive sea level coastal anomaly; a geostrophically balanced northward-flowing coastal jet during

fall and winter; and a depression of sea level with associated southward coastal flow during spring and summer. These seasonal coastal sea level anomalies are also confirmed by satellite altimeter and tide gauge data (Saraceno et al. 2014). The remarkable seasonal changes in surface salinity are associated with redistribution of the large freshwater discharges from the RP derived from in situ and satellite observations (Piola et al. 2000, 2008b; Möller Jr et al. 2008; Guerrero et al. 2014). During the winter months, northward, downwelling favorable winds generate northward currents and onshore Ekman transport (Meccia et al. 2013; Saraceno et al. 2014; Strub et al. 2015) that traps the RP plume near the coast (Palma et al. 2008). Though the northward plume penetrations in winter exhibit significant interannual variations, on average, the plume is positioned near Cape Santa Marta Grande (Fig. 1a). Relaxation of the winter winds allows some of the freshwater to leave the shelf in filaments that extend into the BC (Piola et al. 2008a; Matano et al. 2014), where the low-salinity signal is rapidly diluted by mixing with the salty upper layer carried by the BC. During summer, poleward winds create upwelling and poleward currents, causing freshwater to move south and offshore into the Brazil/Malvinas Confluence (Guerrero et al. 2014; Matano et al. 2014). The RP plume strengthens the inner and mid-shelf currents during fall and early winter. In summer, models show the development of a subsurface northward countercurrent in the mid-shelf, which flows against the prevailing winds (Palma et al. 2008). This countercurrent is presumably responsible for the northward extension of SASW to about 33°S in summer required to sustain the sharp thermohaline gradients across the STSF (Piola et al. 2008a). The summer geostrophic circulation derived from altimetry also shows a southward flow along the inner shelf and a weak northward flow along the outer shelf extending to about 34°S (Saraceno et al. 2014; Strub et al. 2015). Palma et al. (2008) attribute this northward flow to cross-shelf pressure gradients established farther south by the MC that spread northward well beyond the northernmost reach of the MC, as an arrested topographic wave (Csanady 1978).

Off the RP estuary, the CS is characterized by a persistent off-shelf mass flux. Model-derived volume balances of the shelf region between 34°S and 38°S show an annual mean off-shelf transport of ~1.21 Sv (Matano et al. 2014; see also Mendonça et al. 2017). Most of this transport is drawn from SASW from the Patagonian Shelf (1.15 Sv), with very small contributions from the RP discharge and the northern shelf region. The seasonal variations of the off-shelf transport are relatively small and out of phase with the variations of the southern mass flux; it decreases during the winter and increases during the summer (Matano et al. 2014). These results are in agreement with flow patterns inferred using satellite salinity (Guerrero et al. 2014) and the geostrophic velocities derived from altimetry (Strub et al. 2015).

4.3 South Brazil Bight (SBB)

The mean circulation in the middle and outer shelf north of Cape Santa Marta Grande is mostly southwestward and presents significant cross-shelf and seasonal variations in magnitude (Castro and Miranda 1998; Palma and Matano 2009).

Currents in the mid- and outer shelf are stronger in summer and weaker in winter (Matano et al. 2010). These seasonal variations are particularly strong in the inner shelf, where the circulation is driven by baroclinic effects and local winds. Numerical models suggest that the circulation is primarily driven by the poleward flow of the BC in the middle and outer shelf (Palma and Matano 2009), while wind forcing is also important in the inner and middle shelf (Stech and Lorenzzetti 1992). Observations also indicate that the wind stress is a major forcing in the middle shelf region (Dottori and Castro 2009; Dottori and Castro 2018). The influence of remote forcing is manifested in the SST gradients near the shelf break (Campos et al. 2000; Castelão et al. 2004) but is not confined to the surface or to the shelf break, as SACW intrusions and continental shelf waves are additional sources of variability (Castro and Lee 1995; Campos et al. 2010; Filippo et al. 2012; Dottori and Castro 2018). The strongest influence of the BC is observed at depth, where the bottom layer of the outer and middle shelf is permeated by the inflow of SACW throughout the year (Castro and Miranda 1998; Matano et al. 2010). In summer the SACW intrusions extend further onshore (Castro 2014).

The characteristics of the upwelling regime in the SBB are also confirmed by the distribution and variability of passive tracers included in model simulations (Combes and Matano 2014). A large amount of a tracer initially located in the offshore portion of the BC between 25 and 29°S stays offshore and moves south until it meets the MC and leaks offshore in the Brazil/Malvinas Confluence. The remaining part reappears next to the coast as far south as 32°S, transported by the combined action of bottom-layer shelf break upwelling and northeasterly winds (Palma and Matano 2009; Campos et al. 2013). The surface concentration increases at the end of winter when the surface wind stress shifts from downwelling to upwelling favorable and reaches its maximum during spring and summer. A tracer released over the shelf north of ~27°S stays over the shelf but extends just slightly past the 200 m isobath moving south to ~32°S, where it mixes with water from the RP and moves offshore into the Brazil/Malvinas Confluence (Combes and Matano 2014).

5   Surface Chlorophyll *a* Distribution

Satellite observations of chlorophyll *a* distributions reveal the high primary productivity levels of the southwestern South Atlantic shelf (Fig. 1c, see Longhurst 1998; Saraceno et al. 2005; Rivas et al. 2006; Romero et al. 2006; Signorini et al. 2006; Marrari et al. 2013). The largest concentrations are observed close to sediment laden continental discharges such as the RP and along the PS shelf break. Though the RP is a source of nutrients, which may lead to significant blooms in the outer estuary (Calliari et al. 2005; Carreto et al. 2008), global chlorophyll *a* algorithms, such as the one used in this study, frequently overestimate the chlorophyll *a* concentration in these optically complex waters (e.g., Garcia et al. 2005). Thus, the satellite-derived chlorophyll *a* distribution in these regions should be interpreted with caution. South of 38°S, the austral summer chlorophyll *a* distribution suggests

a close association between productive regions and semipermanent frontal systems. In austral summer, the shelf break front emerges as an extended band of high concentrations (generally higher than 3 mg m^{-3}, Fig. 1c). In situ chlorophyll *a* estimates in the shelf break front indicate concentrations exceeding 15 mg m^{-3} and are in overall agreement with the high concentrations indicated by satellite observations (e.g., Garcia et al. 2008; Lutz et al. 2010; Carreto et al. 2016). On average, the shelf break bloom initiates in September and remains high (~ 3.5 mg m^{-3}) until March, though there is substantial interannual variability (Saraceno et al. 2005; Romero et al. 2006; Signorini et al. 2006; Piola et al. 2010). In contrast, the spring bloom in mid-shelf regions decays monotonically after it peaks in October–November (e.g., Carreto et al. 1995; Romero et al. 2006). Enhanced vertical circulation and mixing intense enough to overcome the strong summer stratification, such as might be expected close to ocean fronts, appear to be essential to maintain productivity after the spring bloom. Consequently, in summer regions of enhanced surface chlorophyll concentration (Fig. 1c) are closely associated with weakened vertical stratification (Fig. 2b).

The high chlorophyll *a* concentrations associated with the Valdes tidal front reach a spring-summer maximum of ~3.4 mg m^{-3}. This frontal bloom peaks in January and decays monotonically until May (Romero et al. 2006). Chlorophyll blooms are also observed along an extensive band offshore from the 100 m isobath at 85–150 km from shore between 46 and 52°S. This high chlorophyll *a* band is closely associated with the cold estuarine front (see Fig. 1b, c). The highest satellite chlorophyll *a* concentrations in the latter region can exceed 30 mg m^{-3}, and similarly high in situ estimates have been reported off Grande Bay near 51°S (Lutz et al. 2010; Gómez et al. 2011). This extensive mid-shelf region in southern Patagonia blooms in January, and the chlorophyll *a* concentration decays at about the same rate as the Valdes and shelf break fronts (Romero et al. 2006).

In the SBB, onshore intrusions of SACW combined with wind- and BC eddy-induced upwelling are the primary sources of nutrients leading to nearshore blooms (see Sect. 1.3). In addition to wind-induced upwelling (e.g., Campos et al. 2013), the northward intrusions of RP waters in winter appear to play a significant role in fertilizing the CS (e.g., Ciotti et al. 1995). In contrast to the PS, where shelf break upwelling and tidal and wind mixing are permanent sources of nutrients to the upper layer at specific locations, the nutrient sources in the CS and the SBB are modulated by synoptic atmospheric and oceanic processes. The impact of these episodic upwelling events is not readily apparent in long-term surface chlorophyll *a* climatologies, such as the one presented in Fig. 1c. Consequently, in the two northern regions, the satellite-derived chlorophyll *a* concentration is significantly lower than in the PS. Given the seasonality of alongshore component of wind stress in the CS, the wind-induced upwelling is more frequent in austral summer, when the region is under the influence of upwelling-favorable northeasterly winds (see Campos et al. 2013; Ito et al. 2016). The contrasting chlorophyll *a* distributions between the different shelf regions are displayed by the long-term annual mean concentrations in the SBB, CS, and PS, 1.37 ± 0.48, 3.58 ± 0.81, and 2.15 ± 0.39 mg m^{-3}, respectively. The high areal mean chlorophyll *a* estimated over the CS reflects the influ-

ence of high concentration associated with the RP plume, even after limiting the calculation to concentrations lower than 5 mg m^{-3}. Though in situ data support a high chlorophyll *a* associated with the RP plume (Garcia et al. 2006; Martinez et al. 2005), the mean value in the CS should be interpreted with caution.

6   Surface Ocean CO_2 Fluxes

Analysis of historical partial pressure of CO_2 (pCO_2) is based on data extracted from the SOCAT.v4 data set. Based on the partial pressure and wind data, and using the Wanninkhof (2014) flux parameterization, the sea-air CO_2 fluxes were estimated in the PS (see Kahl et al. 2017). Preliminary estimates in the PS and the MC regions indicate an oceanic annual averaged CO_2 uptake of -8.1×10^{-3} mol m^{-2} d^{-1} (the minus sign indicates flux from the atmosphere to the ocean). The flux is maximum during the austral spring, with an average of -18.6×10^{-3} mol m^{-2} d^{-1}. These fluxes are among the highest CO_2 uptake per unit area in the world ocean, for instance, doubling the CO_2 sink in the North Sea (Thomas et al. 2004). In particular, the PS shelf break front presents intense CO_2 fluxes into the ocean, with an annual mean of -15×10^{-3} mol m^{-2} d^{-1}. The PS shelf break also presents a large seasonal flux variability, reaching -22.3×10^{-3} mol m^{-2} d^{-1} during spring and -4.8×10^{-3} mol m^{-2} d^{-1} in winter. These new estimates of surface CO_2 fluxes in the PS are higher than previously reported (e.g., Bianchi et al. 2009; Padin et al. 2010; Kahl et al. 2017) due to the substantial increase in observations collected during the past decade. Kahl et al. (2017) suggest that biological processes dominate the CO_2 variability in the shelf break region and that the decreased CO_2 sink during winter is mainly due to the decline in biological activity combined with winter convection. The studies in the PS therefore concluded that vertical stratification plays a key role in CO_2 dynamics.

In contrast with the PS, the subtropical shelf off the Brazilian coast acts as a source of CO_2 to the atmosphere (Ito et al. 2005; Padin et al. 2010). Observations conducted in the SBB in November 1997 and January/February and June 1998 indicate net sea-air CO_2 fluxes between 0.3 and 9.8×10^{-3} mol m^{-2} day^{-1} which decrease to ~0.4 and 3.7×10^{-3} mol m^{-2} day^{-1} over the slope and neighboring deep ocean (Ito et al. 2005). Upwelling events observed primarily in summer and biological regenerative processes are thought to play a key role in the CO_2 dynamics in this region (Ito et al. 2005). Observations in the mid- and outer CS collected during 2000–2008 suggest that in austral spring, most of the region acts as a CO_2 sink, while during the fall, the region is characterized by the sharp transition from atmospheric CO_2 source along the coast of southern Brazil to CO_2 sink off the RP mouth (Padin et al. 2010). More recent observations collected in austral spring 2010 and early summer 2011 in the southern SBB and northern CS indicate that shelf waters are a source of CO_2 to the atmosphere (Ito et al. 2016). In late spring the surface CO_2 fluxes in the northern CS vary between 0.5 and 1×10^{-3} mol CO_2 m^{-2} day^{-1} and decrease offshore. The highest fluxes in this region exceed 3×10^{-3} mol CO_2 m^{-2} day^{-1} in the upwelling

region off Cape Santa Marta Grande (Ito et al. 2016). The late summer observations in the northern SBB present much higher CO_2 flux estimates, exceeding 15×10^{-3} mol CO_2 m^{-2} day^{-1} (Ito et al. 2016).

Results from an eddy-resolving, regional ocean biogeochemical model are in good overall agreement with observations, confirming that south of 30° S the western South Atlantic shelf acts as a sink of atmospheric CO_2 (Arruda et al. 2015). The model indicates a weak source of CO_2 to the atmosphere in the SBB. Observed near shore to offshore and meridional pCO_2 gradients are well represented in the simulation. A sensitivity analysis shows that the biological production and solubility are the main processes regulating the model pCO_2, with biological production being particularly important over the continental shelves.

References

Acha EM, Mianzán HW, Guerrero RA et al (2004) Marine fronts at the continental shelves of austral South America. Physical and ecological processes. J Mar Syst 44:83–105

Amor CC (2004) Intrusões da Água Central do Atlântico Sul sobre a Plataforma Continental situada entre a Ilha de São Sebastião (SP) e o Cabo de São Tomé (RJ). Dissertation, Universidade de São Paulo

Arruda R, Calil PHR, Bianchi AA et al (2015) Air-sea CO_2 fluxes and the controls on ocean surface pCO_2 variability in the coastal and open-ocean southwestern Atlantic Ocean: a modeling study. Biogeosciences 12:5793–5809

Bianchi AA, Massonneau M, Olivera RM (1982) Análisis estadístico de las características T-S del sector austral de la plataforma continental argentina. Acta Oceanogr Argent 3(1):93–118

Bianchi AA, Bianucci L, Piola AR et al (2005) Vertical stratification and air-sea CO2 fluxes in the Patagonian shelf. J Geophys Res Oceans 110(7):1–10

Bianchi AA, Ruiz-Pino D, Isbert Perlender H et al (2009) Annual balance and seasonal variability of sea-air CO_2 fluxes in the Patagonia Sea: their relationship with fronts and chlorophyll distribution. J Geophys Res 114:C03018. https://doi.org/10.1029/2008JC004854

Borús J, Uriburu Quirno M, Calvo D (2017) Evaluación de caudales diarios descargados por los grandes ríos del Sistema del Plata al estuario del Río de la Plata. Dirección de Sistemas de Información y Alerta Hidrológico. Instituto Nacional del Agua, Ezeiza

Brandhorst W, Castello JP (1971) Evaluación de los recursos de anchoíta (Engraulis anchoita) frente a la Argentina y Uruguay. I. Las condiciones oceanográficas, sinopsis del conocimiento actual sobre la anchoíta y el plan para su evaluación. Proy Des Pesq FAO 29: 63 pp. Mar del Plata

Calliari D, Gómez M, Gómez N (2005) Biomass and composition of the phytoplankton in the Río de la Plata: large-scale distribution and relationship with environmental variables during a spring cruise. Cont Shelf Res 25:197–210

Campos EJ, Goncalves J, Ikeda Y (1995) Water mass characteristics and geostrophic circulation in the South Brazil Bight: summer of 1991. J Geophys Res 100:18537–18550

Campos EJD, Lentini CAD, Miller JL et al (1999) Interannual variability of the sea surface temperature in the South Brazil Bight. Geophys Res Lett 26:2061–2064

Campos EJ, Velhote D, da Silveira IC (2000) Shelf break upwelling driven by Brazil current cyclonic meanders. Geophys Res Lett 27(6):751–754

Campos PC, Möller Jr OO, Piola AR (2013) Seasonal variability and coastal upwelling near Cape Santa Marta (Brazil). J Geophys Res Oceans 118:1420–1433. https://doi.org/10.1002/jgrc.20131

Carranza MM, Gille ST, Piola AR et al (2017) Wind modulation of upwelling at the shelf-break front off Patagonia: observational evidence. J Geophys Res Oceans 122(3):2401–2421

Carreto JI, Lutz VA, Carignan MO et al (1995) Hydrography and chlorophyll-a in a transect from the coast to the shelf-break in the Argentinean Sea. Cont Shelf Res 15:315–336

Carreto JI, Montoya N, Akselman R et al (2008) Algal pigment patterns and phytoplankton assemblages in different water masses of the Río de la Plata maritime front. Cont Shelf Res 28:1589–1606

Carreto JI, Montoya NG, Carignan MO et al (2016) Environmental and biological factors controlling the spring phytoplankton bloom at the Patagonian shelf-break front– degraded fucoxanthin pigments and the importance of microzooplankton grazing. Prog Oceanogr 146:1–21

Castelão RM (2012) Sea surface temperature and wind stress curl variability near a cape. J Phys Oceanogr 42:2073–2087

Castelão RM, Barth JA (2006) Upwelling around Cabo Frio, Brazil: the importance of wind stress curl. Geophys Res Lett 33:L03602. https://doi.org/10.1029/2005GL025182

Castelão RM, Campos EJD, Miller JL (2004) A modelling study of coastal upwelling driven by wind and meanders of the Brazil current. J Coast Res 20(3):662–671

Castello JP, Möller OO (1977) Sobre as condições oceanográficas no Rio Grande do Sul. Atlantica 2:1–119

Castro BM, Lee TN (1995) Wind-forced sea level variability on the southeast Brazilian shelf. J Geophys Res 100(C8):16,045–16,056

Castro BM (2014) Summer/winter stratification variability in the central part of the South Brazil bight. Cont Shelf Res 89:15–26

Castro BM, Miranda LB (1998) Physical oceanography of the western Atlantic continental shelf located between 4°N and 34°S. In: Robinson AR, Brink KH (eds) The sea, vol 11. Wiley, New York, pp 209–251

Castro BM, Lorenzetti JA, Silveira ICA et al (2006) O Ambiente Oceanográfico da Plataforma Continental e do Talude na Região Sudeste-Sul do Brasil, 1st edn. Edusp, p 11–120

Cerda C, Castro BM (2014) Hydrographic climatology of South Brazil Bight shelf waters between São Sebastião (24°S) and Cabo São Tomé (22°S). Cont Shelf Res 89:5–14

Ciotti AM, Odebrecht C, Fillmann G et al (1995) Freshwater outflow and subtropical convergence influence on phytoplankton biomass on the southern Brazilian continental shelf. Cont Shelf Res 15:1737–1756

Cirano M, Campos EJ (1996) Numerical diagnostic of the circulation in the Santos Bight with COROAS hydrographic data. Rev Bras Oceanogr 44(2):105–101

Combes V, Matano RP (2014) A two-way nested simulation of the oceanic circulation in the Southwestern Atlantic. J Geophys Res Oceans 119. https://doi.org/10.1002/2013JC009498

Csanady GT (1978) The arrested topographic wave. J Phys Oceanogr 8:47–62

Dávila PM, Figueroa D, Müller E (2002) Freshwater input into the coastal ocean and its relation with salinity distribution off austral Chile (35–55°S). Cont Shelf Res 22:521–534

Depetris PJ, Kempe S, Latif M et al (1996) ENSO-controlled flooding in the Parana River (1904–1991). Naturwiss 83:127–129

Dottori M, Castro BM (2009) The response of the Sao Paulo continental shelf, Brazil, to synoptic-winds. Ocean Dynam 59:603–614

Dottori M, Castro BM (2018) The role of remote wind forcing in the subinertial current variability in the central and northern parts of the South Brazil Bight. Ocean Dynam, 68: 677, https://doi.org/10.1007/s10236-018-1153-9

Emilsson I (1961) The shelf and coastal waters off southern Brazil. Bol Inst Oceanogr 11(2):101–112

Filippo A, Kjerfve B, Torres AR et al (2012) Low-frequency variability of sea level along the Mid-Atlantic Coast of South America, in 1983. Rev Bras Geofis 30(1):5–14

Franchito SH, Oda TO, Rao VB et al (2008) Interaction between coastal upwelling and local winds at Cabo Frio, Brazil: an observational study. J Appl Meteorol Climatol 47:1590–1598

Franco BC, Piola AR, Rivas AL et al (2008) Multiple thermal fronts near the Patagonian shelf break. Geophys Res Lett 35(2):L02607. https://doi.org/10.1029/2007GL032066

Garcia CAE, Garcia VM, McClain CR (2005) Evaluation of SeaWiFS chlorophyll algorithms in the Southwestern Atlantic and Southern Oceans. Remote Sens Environ 95:125–137

Garcia VMT, Signorini S, Garcia CAE et al (2006) Empirical and semi-analytical chlorophyll algorithms in the South-Western Atlantic coastal region (25–40°S and 60–45°W). Int J Remote Sens 27(8):1539–1562. https://doi.org/10.1080/01431160500382857

Garcia VMT, Garcia CAE, Mata MM et al (2008) Environmental factors controlling the phytoplankton blooms at the Patagonia shelf-break in spring. Deep-Sea Res I 55:1150–1166

Glorioso PD (1987) Temperature distribution related to shelf-sea fronts on the Patagonian shelf. Cont Shelf Res 7(1):27–34

Gómez MI, Piola AR, Kattner G et al (2011) Biomass of autotrophic dinoflagellates under weak vertical stratification and contrasting chlorophyll levels in subantarctic shelf water. J Plankton Res 33(8):1304–1310

Guerrero RA, Piola AR (1997) Masas de agua en la plataforma continental. In: Boschi EE (ed) El Mar Argentino y sus Recursos Pesqueros: Antecedentes Históricos de las Exploraciones en el Mar y las Características Ambientales, vol. 1. Instituto Nacional de Investigación y Desarrollo Pesquero, Mar del Plata, pp 107–118

Guerrero R, Piola AR, Fenco H et al (2014) The salinity signature of the cross-shelf exchanges in the southwestern Atlantic Ocean: satellite observations. J Geophys Res Oceans 119. https://doi.org/10.1002/2014JC010113

Ito R, Schneider B, Thomas H (2005) Distribution of surface pCO_2 and air–sea fluxes in the Southwestern subtropical Atlantic and adjacent continental shelf. J Mar Syst 56:227–242. https://doi.org/10.1016/j.jmarsys.2005.02.005

Ito RG, Garcia CAE, Tavano VM (2016) Net sea-air CO_2 fluxes and modelled pCO_2 in the southwestern subtropical Atlantic continental shelf during spring 2010 and summer 2011. Cont Shelf Res 119(Suppl C):68–84. https://doi.org/10.1016/j.csr.2016.03.013

Kahl LC, Bianchi AA, Osiroff AP et al (2017) Distribution of sea-air CO_2 fluxes in the Patagonian Sea: seasonal, biological and thermal effects. Cont Shelf Res 143:18–28

Lentini CAD, Podestá GG, Campos EJD et al (2001) Sea surface temperature anomalies on the Western South Atlantic from 1982 to 1994. Cont Shelf Res 21:89–112

Longhurst A (1998) Ecological geography of the sea. Academic Press, San Diego

Lucas AJ, Guerrero RA, Mianzán HW et al (2005) Coastal oceanographic regimes of the northern argentine continental shelf (34–43°S). Estuar Coast Shelf Sci 65:405–420

Lutz VA, Segura V, Dogliotti AI et al (2010) Primary production in the argentine sea during spring estimated by field and satellite models. J Plankton Res 32:181–195. https://doi.org/10.1093/plankt/fbp117

Marrari M, Signorini S, McClain CR et al (2013) Reproductive success of the Argentine anchovy, Engraulis anchoita, in relation to environmental variability at a mid-shelf front (Southwestern Atlantic Ocean). Fish Oceanogr 22:247–261

Marrari M, Piola AR, Valla D (2017) Variability and 20-year trends in satellite-derived surface chlorophyll concentrations in large marine ecosystems around South and Western Central America. Front Mar Sci. https://doi.org/10.3389/fmars.2017.00372

Martinez G, Brugnoli E, Hernandez J et al (2005) How valid is the SeaWiFS estimation of chlorophyll-a at the Rio de la Plata estuary and its area of influence? Proc SPIE 5656. Active and Passive Remote Sensing of the Oceans. https://doi.org/10.1117/12.582665

Martos P, Piccolo MC (1988) Hydrography of the Argentine continental shelf between 38 and 42 S. Cont Shelf Res 8:1043–1056

Matano RP, Palma ED (2008) The upwelling of downwelling currents. J Phys Oceanogr 38:2482–2500. https://doi.org/10.1175/2008JPO3783.1

Matano RP, Palma ED, Piola AR (2010) The influence of the Brazil and Malvinas currents on the Southwestern Atlantic shelf circulation. Ocean Sci 6:983–995

Matano RP, Combes V, Piola AR et al (2014) The salinity signature of the cross-shelf exchanges in the southwestern Atlantic Ocean: numerical simulations. J Geophys Res Oceans 119. https://doi.org/10.1002/2014JC010116

Meccia VL, Simionato CG, Guerrero RA (2013) The Río de la Plata estuary response to wind variability in synoptic timescale: salinity fields and salt wedge structure. J Coast Res 29(1):61–77

Mendonça LF, Souza RB, Aseff CRC et al (2017) Regional modeling of the water masses and circulation annual variability at the southern Brazilian continental shelf. J Geophys Res 122:1232–1253

Miller RN, Matano RP, Palma ED (2011) Shelfbreak upwelling induced by alongshore currents: analytical and numerical results. J Fluid Mech 686:239–249. https://doi.org/10.1017/jfm.2011.326

Miranda LB (1985) Correlacão T-S de Massas de água das regiões costeira e oceânica entre o Cabo de São Tomé (RJ) e a Ilha de São Sebastião (SP), Brasil. Bol Inst Oceanogr Univ São Paulo 33(2):105–119

Möller Jr OO, Piola AR, Freitas AC et al (2008) The effects of river discharge and seasonal winds on the shelf off southeastern South America. Cont Shelf Res 28(13):1607–1624

Moreira D, Simionato CG, Dragani W (2011) Modeling ocean tides and their energetics in the North Patagonia gulfs of Argentina. J Coast Res 27(1):87–102

Nagai RH, Sousa SHM, Mahiques MM (2014) The Southern Brazilian shelf. Geol Soc Lond Mem 41:47–54

O'Reilly JE, Maritorena S, O'Brien MC et al (2000) SeaWiFS postlaunch calibration and validation analyses: Part 3. SeaWiFS postlaunch technical report series. In: Hooker SB, Firestone RE (eds) NASA Tech. Memo 2000–206892, 11

Padin XA, Vázquez-Rodríguez M, Castaño M et al (2010) Air-Sea CO_2 fluxes in the Atlantic as measured during boreal spring and autumn. Biogeosciences 7:15871606

Palma ED, Matano RP (2009) Disentangling the upwelling mechanisms of the South Brazil bight. Cont Shelf Res. https://doi.org/10.1016/j.csr.2009.04.002

Palma ED, Matano RP (2012) A numerical study of the Magellan plume. J Geophys Res 117:C05041. https://doi.org/10.1029/2011JC007750

Palma ED, Matano RP, Piola AR (2004) A numerical study of the Southwestern Atlantic shelf circulation: Barotropic response to tidal and wind forcing. J Geophys Res 109:C08014. https://doi.org/10.1029/2004JC002315

Palma ED, Matano RP, Piola AR (2008) A numerical study of the southwestern Atlantic shelf circulation: Stratified Ocean response to local and offshore forcing. J Geophys Res Oceans 113(11):C11010. https://doi.org/10.1029/2007JC004720

Pimenta F, Garvine RW, Munchow A (2008) Observations of coastal upwelling off Uruguay downshelf of the Plata estuary, South America. J Mar Res 66:835–872

Piola AR, Matano RP (2017) Ocean currents: Atlantic western boundary—Brazil current/Falkland (Malvinas) current. Reference module in earth systems and environmental sciences, Elsevier, doi: https://doi.org/10.1016/B978-0-12-409548-9.10541-X

Piola AR, Campos EJD, Möller OO Jr et al (2000) Subtropical shelf front off eastern South America. J Geophys Res 105(C3):6565–6578

Piola AR, Matano RP, Palma ED et al (2005) The influence of the Plata River discharge on the western South Atlantic shelf. Geophys Res Lett. https://doi.org/10.1029/2004GL021638

Piola AR, Möller OO, Guerrero RA et al (2008a) Variability of the subtropical shelf front off eastern South America: winter 2003 and summer 2004. Cont Shelf Res 28:1639–1648

Piola AR, Romero SI, Zajaczkovski U (2008b) Space-time variability of the Plata plume inferred from ocean color. Cont Shelf Res 28:1556–1567

Piola AR, Martínez Avellaneda N, Guerrero RA et al (2010) Malvinas-slope water intrusions on the northern Patagonia continental shelf. Ocean Sci 6(1):345–359

Pisoni JP, Rivas AL, Piola AR (2015) On the variability of tidal fronts on a macrotidal continental shelf, northern Patagonia, Argentina. Deep Sea Res II Top Stud Oceanogr 119:61–68

Proença LAO, Schramm MA, Alves TP, et al (2017) The extraordinary 2016 autumn DSP outbreak in Santa Catarina, South Brazil, explained by large-scale oceanographic processes, Proc 16 Int Conf Harm Algae, Proença LAO, Hallegraeff GM (Eds), Int Soc for the Study of Harmful Algae and Intergovernmental Oceanographic Commission, Brazil, 42–45

Reynolds RW, Smith TM, Liu C et al (2007) Daily high-resolution-blended analyses for sea surface temperature. J Clim 20:5473–5496

Rivas AL (1997) Current meter observations in the argentine continental shelf. Cont Shelf Res 17:391–406. https://doi.org/10.1016/S0278-4343(96)00039-8

Rivas AL, Pisoni JP (2010) Identification, characteristics and seasonal evolution of surface thermal fronts in the Argentinean continental shelf. J Mar Syst 79(1–2):134–143

Rivas AL, Dogliotti AI, Gagliardini DA (2006) Satellite-measured surface chlorophyll variability in the Patagonian shelf. Cont Shelf Res. https://doi.org/10.1016/j.csr.2006.01.013

Robertson AW, Mechoso CR (1998) Interannual and decadal cycles in river flows of southeastern South America. J Clim 11:2570–2581

Rodrigues RR, Lorenzetti JA (2001) A numerical study of the effects of bottom topography and coastline geometry on the southeast Brazilian coastal upwelling. Cont Shelf Res 21:371–393

Romero SI, Piola AR, Charo M et al (2006) Chlorophyll-a variability off Patagonia based on SeaWiFS data. J Geophys Res 111:C05021

Ruiz-Etcheverry LA, Saraceno M, Piola AR et al (2016) Sea level anomaly on the Patagonian continental shelf: trends, annual patterns and geostrophic flows. J Geophys Res Oceans 121:2733–2754. https://doi.org/10.1002/2015JC011265

Sabatini M, Reta R, Matano R (2004) Circulation and zooplankton biomass distribution over the southern Patagonian shelf during late summer. Cont Shelf Res 24:1359–1373

Saraceno MC, Provost C, Piola AR et al (2004) Brazil Malvinas frontal system as seen from 9 years of advanced very high resolution radiometer data. J Geophys Res Oceans 109(5):C05027. https://doi.org/10.1029/2003JC002127

Saraceno MC, Provost C, Piola AR (2005) On the relationship between satellite-retrieved surface temperature fronts and chlorophyll a in the western South Atlantic. J Geophys Res Oceans 110(11):1–16. https://doi.org/10.1029/2004JC002736

Saraceno M, Simionato CG, Ruiz Etcheverry LA (2014) Sea surface height trend and variability at seasonal and interannual time scales in the Southeastern South American continental shelf between 27°S and 40°S. Cont Shelf Res 91:82–94. https://doi.org/10.1016/j.csr.2014.09.002

Scasso LM, Piola AR (1988) Intercambio neto de agua entre el mar y la atmósfera en el Golfo San Matías. Geoacta 15(1):13–31

Signorini SR, Garcia VMT, Piola AR et al (2006) Seasonal and interannual variability of calcite in the vicinity of the Patagonian shelf break (38°S–52°S). Geophys Res Lett 3:L16610. https://doi.org/10.1029/2006GL026592

Silveira ICA, Schmidt ACK, Campos EJD et al (2000) A Corrente do Brasil ao Largo da Costa Leste Brasileira. Rev Bras Oceanogr 48:171–183

Simionato CG, Nuñez MN, Engel M (2001) The salinity front of the Río de la Plata–a numerical case study for winter and summer conditions. Geophys Res Lett 28(13):2641–2644

Simionato CG, Clara Tejedor ML, Campetella C et al (2010) Patterns of sea surface temperature variability on seasonal to sub-annual scales at and offshore the Río de la Plata estuary. Cont Shelf Res 30(19):983–997

Souza RB, Robinson IS (2004) Lagrangian and satellite observations of the Brazilian coastal current. Cont Shelf Res 24:241–262

Stech JL, Lorenzzetti JA (1992) The response of the South Brazil Bight to the passage of wintertime cold fronts. J Geophys Res 97(C6):9507–9520

Stevenson MR, Dias-Brito D, Stech JL et al (1998) How do cold water biota arrive in a tropical bay near Rio de Janeiro, Brazil? Cont Shelf Res 18(13):1595–1612

Strub PT, James C, Combes V et al (2015) Altimeter-derived seasonal circulation on the Southwest Atlantic shelf: 27°–43°S. J Geophys Res Oceans. https://doi.org/10.1002/2015JC010769

Thomas H, Bozec Y, Elkalay K et al (2004) Enhanced open ocean storage of CO_2 from shelf sea pumping. Science 304:1005–1008

Tonini MH, Palma ED, Piola AR (2013) A numerical study of gyres, thermal fronts and seasonal circulation in austral semi-enclosed gulfs. Cont Shelf Res 65:97–110

Valla D, Piola AR (2015) Evidence of upwelling events at the northern Patagonian shelf break. J Geophys Res Oceans 120:7635–7656

Wanninkhof R (2014) Relationship between wind speed and gas exchange over the ocean revisited. Limnol Oceanogr Methods 12(6):351–362

Zavialov PO, Möller OO Jr, Campos EJD (2002) First direct measurements of currents on the continental shelf of southern Brazil. Cont Shelf Res 22:1975–1986. https://doi.org/10.1016/S0278-4343(02)00049-3